Biophysical Letter

# Cell Volume Fluctuations in MDCK Monolayers

Steven M. Zehnder,[1] Melanie Suaris,[2] Madisonclaire M. Bellaire,[3] and Thomas E. Angelini[1,4,*]
[1]Department of Mechanical and Aerospace Engineering, [2]J. Crayton Pruitt Family Department of Biomedical Engineering, [3]Department of Physics, and [4]Institute for Cell Engineering and Regenerative Medicine, University of Florida, Gainesville, Florida

ABSTRACT Cells moving collectively in tissues constitute a form of active matter, in which collective motion depends strongly on driven fluctuations at the single-cell scale. Fluctuations in cell area and number density are often seen in monolayers, yet their role in collective migration is not known. Here we study density fluctuations at the single- and multicell level, finding that single-cell volumes oscillate with a timescale of 4 h and an amplitude of 20%; the timescale and amplitude are found to depend on cytoskeletal activity. At the multicellular scale, density fluctuations violate the central limit theorem, highlighting the role of nonequilibrium driving forces in multicellular density fluctuations.

Received for publication 21 August 2014 and in final form 14 November 2014.

*Correspondence: t.e.angelini@ufl.edu

Collective cell motion is essential to tissue development, health, disease, and repair (1–3). To explore the driving forces of cell motion in tissues, monolayers are often investigated (4–7). Motion in monolayers depends strongly on cell number density, and exhibits phase transitions as cell density rises (8–12). Theories of phase transitions and the statistical physics of active matter, including cells, have been investigated thoroughly, and often density fluctuations are strongly coupled to collective motion (13–15). A careful look at published snapshots and videos of cell monolayers reveals large variations in cell area and density fluctuations (6,7,16). However, these fluctuations in cell density and size have not been explored, limiting our understanding of the relationship between single-cell dynamics and collective cell motion.

Here we investigate fluctuations of cell size and spatial distribution in Madin Darby canine kidney (MDCK) cell monolayers. We find that cell volumes fluctuate by $\pm 20\%$, oscillating with a timescale of 4 h. The cytoskeleton's role is observed by inhibiting Myosin II with blebbistatin, which substantially reduces volume fluctuations and increases the oscillation time. We also observe large-scale density fluctuations that violate the central limit theorem, which has not yet been reported in monolayers of cells that form strong cell-cell junctions (17). Estimates of cell permeability show that cell volume fluctuations may involve fluid transport between cells through gap junctions or across the cell membrane. These results suggest that fluid transport associated with cell volume fluctuations may contribute to collective motion in monolayers and tissues.

## Projected area fluctuations

We explore fluctuations in the projected area of MDCK cells with time-lapse microscopy. Monolayers are grown in standard culture conditions described in the Supporting Material. Imaging is performed with an incubation chamber mounted on an inverted microscope. Cell density is visibly heterogeneous in space and time; snapshots show large spatial variations in cell density and manual cell tracking shows large cell size fluctuations in time (Fig. 1, *A–D*).

To measure area fluctuations in large numbers, phase contrast images are thresholded to identify cell boundaries. The position and projected area of each cell is determined by its boundary, and cells are followed in time with tracking software (18). Large fluctuations can be directly seen in cell area traces over time and in time-lapse video (see Fig. S2 and Movie S1). The standard deviation in time of area fluctuations about the mean, averaged over all tracked cells, shows that the typical cell area fluctuates $\pm 20.7\%$ with a standard error of 0.4% ($N = 323$).

To check this result, the nuclei of MDCK cells expressing fluorescent histones are tracked, and a Voronoi tessellation is performed. Approximating each cell area with the area of its Voronoi cell, we find fluctuations of $\pm 17.5\%$ with a standard error of 0.2% ($N = 1038$). A reduced fluctuation is expected for Voronoi cells because Voronoi analysis cannot detect shape changes at cell boundaries. In both cases, treatment with 100 $\mu$M blebbistatin, a Myosin II inhibitor, reduces fluctuations by ~50%; in phase-contrast analysis, the fluctuations are $10.1 \pm 0.2\%$ ($N = 1015$) and in Voronoi analysis, they are $9.4 \pm 0.2\%$ ($N = 1014$). Replacing blebbistatin with standard growth media yields a recovery of fluctuations within 2 h. These results suggest that the cytoskeleton drives cell area fluctuations, although

Editor: Cecile Sykes.

http://dx.doi.org/10.1016/j.bpj.2014.11.1856

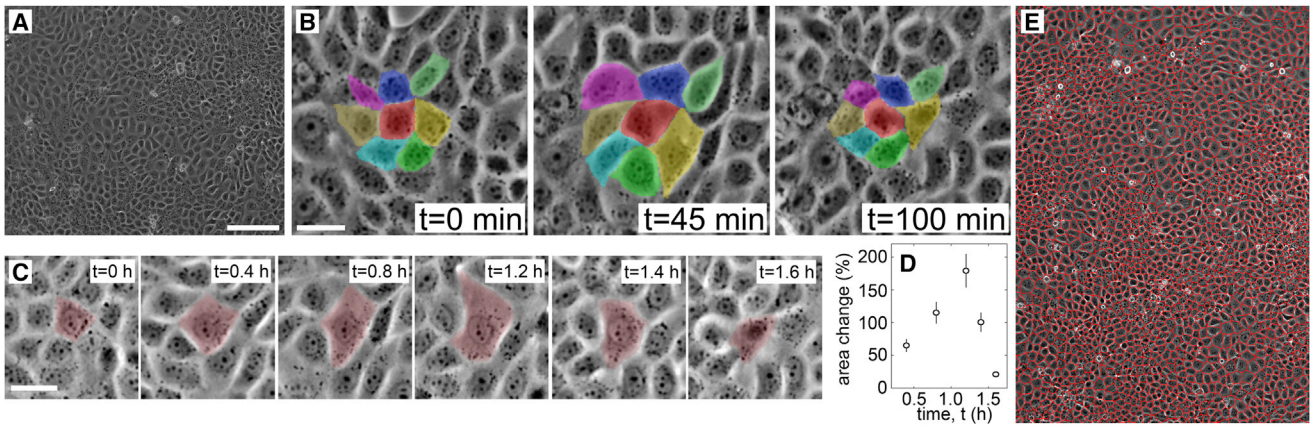


**FIGURE 1** (*A*) Monolayers have large spatial variations in projected cell area; 150-$\mu$m scale bar. (*B*) Cell groups fluctuate together in time. Each color marks the same cell at different times; 30-$\mu$m scale bar. (*C* and *D*) Single cells can fluctuate by ~200% relative to their minimum area; 30-$\mu$m scale bar. (*E*) Cell areas are measured with a Voronoi tessellation based on nucleus locations. To see this figure in color, go online.

other cytoskeletal treatments like Rac1 inhibition or actin depolymerization with cytochalasin will further reveal underlying mechanisms.

## Thickness and tilt fluctuations

To test whether cells fluctuate in thickness, we perform confocal microscopy measurements, collecting stacks over time. Cells are fluorescently dyed with 5-chloromethylfluorescein diacetate, which permeates the cytosol. At each instant in time, the monolayer appears flat. We measure the monolayer thickness by fitting an error function to intensity profiles along the $z$ axis. We use the midpoint of the intensity drop to identify the apical side of the cell, locally, at 1000 random $XY$ locations over an area of 160 $\times$ 160 $\mu$m, covering ~64 cells. The basal location is chosen to be the lowest focal plane in which cell cross-sections are observed, which is constant. We find that the layer is 7.1 $\pm$ 0.7 $\mu$m thick, averaged over space and time (mean $\pm$ standard deviation). To assess how local heights vary in time, we compute a temporal standard deviation of local height and average over all locations in space, yielding a mean fluctuation of 4.8% with a spatial variation of 2.0%. Thus, cell thickness fluctuates by ~340 nm in time. The 95% confidence intervals of the intensity profile fits are ~300 nm, so these fluctuations may be experimental uncertainty limited by sampling frequency along the $z$ axis. We find the same instantaneous spatial variation in height, 4.7%, which varies in time by 1.1%. (Fig. 2, *A–E*).

The cell-cell interface is not perfectly vertical, so we explore interfacial orientation fluctuations. $Z$ projections of confocal stacks show clear boundaries, suggesting that a substantial fraction of cell-cell interfaces is nearly vertical. We determine the orientation of interfaces from $XZ$ slices, when clear boundaries are observed, using IMAGEJ software ($N$ = 110; National Institutes of Health, Bethesda, MD). The histogram of angles is peaked at the vertical orientation, and the cumulative distribution function shows

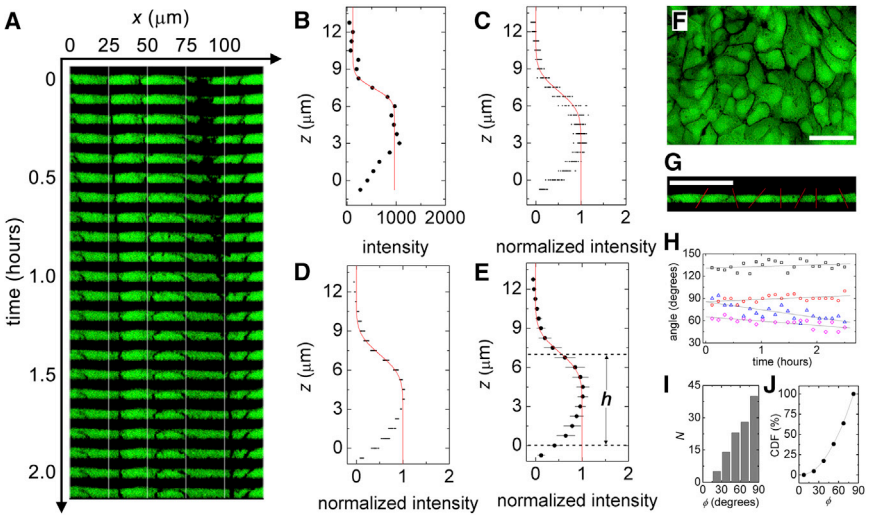


**FIGURE 2** (*A*) *XZ* slices appear flat and boundary angles are steady during motion. (*B*) Intensity traces along the *z* axis are fit at 1000 locations over 2.4 h (one location and time shown; *red line*, fit). (*C*) The overlay of intensity at one location over time shows small variations. (*D*) The overlay of the space-averaged traces also shows small variations. (*E*) Layer thickness averaged over space and time is 7.1 $\pm$ 0.7 $\mu$m. (*F*) *Z* projections show clear boundaries. (*G*) Boundary angles are determined from *XZ* slices. (*H*) Boundaries maintain constant orientation (each dataset is for a different boundary). (*I* and *J*) Angle histogram and cumulative distribution function show that 73% of cell boundaries are oriented within 45° of vertical. (Scale bars = 50 $\mu$m; all *XZ* plots have the same scale along both directions.) To see this figure in color, go online.

that >73% of interfaces are within 45° of vertical; 50% of cells are within 30° of vertical. We estimate the error in assuming vertical walls treating the real cell as a conical cross section, and the approximate cell as a cylinder with a radius equal to that of the midplane of the conical cell. The average cell is 7-$\mu$m thick with a diameter of ~30 $\mu$m; assuming a 30° tilt, the error in volume is ~2%. We also observe that the orientation of cell boundaries remains relatively constant in time (Fig. 2).

### Volume fluctuations in time and space

For cells to conserve volume as they fluctuate in area, they would have to expand in height by 20%. Given the small height and tilt variations observed here, volume fluctuations may be approximated by area fluctuations, $\delta V \approx \delta A$. Simultaneous measurements of cell volume, area, and thickness also support the validity of this approximation (see the Supporting Material). To characterize how cell volumes fluctuate in time, we compute a volume autocorrelation function, $C_{\delta V\text{-}\delta V}$, correlating the approximate volume fluctuations, $\delta V$. We find that $C_{\delta V\text{-}\delta V}$ has a strong negative minimum at $\tau = 2$ h, showing that cell volume oscillates about its mean with a timescale of 4 h. Reducing cytoskeletal contractions with blebbistatin shifts the peak in $C_{\delta V\text{-}\delta V}$ to 3 h, corresponding to a 6 h oscillation. The autospectral density function of volume fluctuations, $S(\omega)$, exhibits peaks corresponding to these oscillation times (Fig. 3 *A*).

Cell volume fluctuations may be linked to the large-scale spatial variations in density seen in monolayers. Frequently seen in active matter systems, the central limit theorem (CLT) is violated (14,15,19). Randomly fluctuating equilibrium variables obey the CLT; in regions containing $N$ particles on average, the number of particles fluctuates like $\sigma \sim N^{1/2}$, where $\sigma$ is the standard deviation of particle number. The CLT is tested by dividing large systems into smaller subsystems, counting particles, and computing $\sigma$ and $N$ over the different subsystems. We test for a CLT violation by identifying all fluorescent nuclei within our field of view, as described above, averaging over 100 frames and roughly 2000 cells in each frame. A plot of $\sigma/N^{1/2}$ demonstrates that cell density fluctuations violate the CLT, with $\sigma \sim N^{5/6}$. To ensure that this result is not due to small sample size, we repeat the calculation on 2000 randomly distributed particles 100 different times, finding no CLT violation.

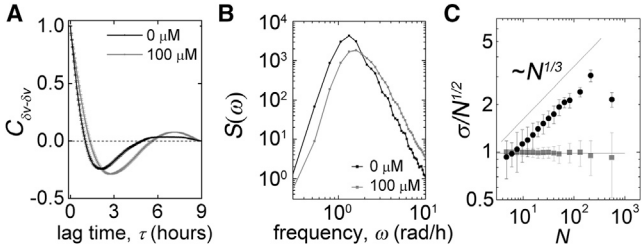


**FIGURE 3 (*A* and *B*) Volume autocorrelation and autospectral density functions show that cell volume oscillates with a period sensitive to blebbistatin treatment. (*C*) Cell density fluctuations in monolayers violate the central limit theorem (*solid circles*, cells; *shaded squares*, random particle).**

## CONCLUSIONS

The volume fluctuations observed here require water transport in and out of the cell. Isolated cells under isotonic conditions maintain a constant volume by regulating their osmotic pressure with ion pumps (20). However, volume regulation in monolayers may differ from the single-cell case, and long timescale reversals of ion transport could drive water in and out of the cell, generating volume changes under isotonic conditions. Typical timescales of volume recovery in response to osmotic pressure, combined with estimates of the hydraulic permeability of single cells, suggest that this mechanism could drive the volume fluctuations observed here (see the Supporting Material).

Another way that cells may change volume is by exchanging fluid with their neighbors through gap junctions. We estimate a cell-cell permeability based on the size and number of gap junctions in MDCK cells, and find that a cell could expel 20% of its own volume in 2 h by generating 1.1 kPa of excess pressure, relative to its neighbors. Comparable levels of spatial variability in cytoskeleton-generated normal stress have been measured in epithelial, endothelial, and cancer cell layers (7). Thus, it is possible that cell volume fluctuations involve cytoskeleton-driven fluid transport though gap junctions. Further estimates of potential permeability limitations of the cytoskeleton itself suggest that the cytoskeletal mesh may not inhibit this very slow flow (see the Supporting Material).

In future work we will manipulate gap junctions and ion channels to explore their relative roles in water transport-associated cell volume fluctuations. Further studies on the relationship between single-cell volume fluctuations and multicellular CLT violations will elucidate the microscopic origins of collective cell migration patterns. Studies of the interplay between contractile cell-generated tension and stress relaxation associated with cell motion or cell division are at the forefront of our growing understanding of collective cell motion. Further exploration of cell volume fluctuations may help to inform discovery in this developing area of research.

## SUPPORTING MATERIAL

Supporting Materials and Methods, four figures, and one movie are available at http://www.biophysj.org/biophysj/supplemental/S0006-3495(14)03068-9.

## ACKNOWLEDGMENTS

This project was funded by National Science Foundation grant No. CMMI-1161967.

## SUPPORTING CITATIONS

References (21–39) appear in the Supporting Material.

## REFERENCES


1. Friedl, P., and D. Gilmour. 2009. Collective cell migration in morphogenesis, regeneration and cancer. *Nat. Rev. Mol. Cell Biol.* 10:445–457.
2. Rørth, P. 2009. Collective cell migration. *Annu. Rev. Cell Dev. Biol.* 25:407–429.
3. Ranft, J., M. Basan, …, F. Jülicher. 2010. Fluidization of tissues by cell division and apoptosis. *Proc. Natl. Acad. Sci. USA.* 107:20863–20868.
4. Trepat, X., M. R. Wasserman, …, J. J. Fredberg. 2009. Physical forces during collective cell migration. *Nat. Phys.* 5:426–430.
5. Poujade, M., E. Grasland-Mongrain, …, P. Silberzan. 2007. Collective migration of an epithelial monolayer in response to a model wound. *Proc. Natl. Acad. Sci. USA.* 104:15988–15993.
6. Puliafito, A., L. Hufnagel, …, B. I. Shraiman. 2012. Collective and single cell behavior in epithelial contact inhibition. *Proc. Natl. Acad. Sci. USA.* 109:739–744.
7. Tambe, D. T., C. C. Hardin, …, X. Trepat. 2011. Collective cell guidance by cooperative intercellular forces. *Nat. Mater.* 10:469–475.
8. Vedula, S. R. K., M. C. Leong, …, B. Ladoux. 2012. Emerging modes of collective cell migration induced by geometrical constraints. *Proc. Natl. Acad. Sci. USA.* 109:12974–12979.
9. Szabó, B., G. J. Szöllösi, …, T. Vicsek. 2006. Phase transition in the collective migration of tissue cells: experiment and model. *Phys. Rev. E Stat. Nonlin. Soft Matter Phys.* 74:061908.
10. Szabó, A., R. Ünnep, …, A. Czirók. 2010. Collective cell motion in endothelial monolayers. *Phys. Biol.* 7:046007.
11. Angelini, T. E., E. Hannezo, …, D. A. Weitz. 2011. Glass-like dynamics of collective cell migration. *Proc. Natl. Acad. Sci. USA.* 108:4714–4719.
12. Vedel, S., S. Tay, …, S. R. Quake. 2013. Migration of cells in a social context. *Proc. Natl. Acad. Sci. USA.* 110:129–134.
13. Toner, J., Y. Tu, and S. Ramaswamy. 2005. Hydrodynamics and phases of flocks. *Ann. Phys.* 318:170–244.
14. Ramaswamy, S. 2010. The mechanics and statistics of active matter. *Annu. Rev. Condens. Matter Phys.* 1:323–345.
15. Marchetti, M., J. Joanny, …, R. A. Simha. 2013. Hydrodynamics of soft active matter. *Rev. Mod. Phys.* 85:1143.
16. Serra-Picamal, X., V. Conte, …, X. Trepat. 2012. Mechanical waves during tissue expansion. *Nat. Phys.* 8:628–634.
17. Duclos, G., S. Garcia, …, P. Silberzan. 2014. Perfect nematic order in confined monolayers of spindle-shaped cells. *Soft Matter.* 10:2346–2353.
18. Crocker, J. C., and D. G. Grier. 1996. Methods of digital video microscopy for colloidal studies. *J. Colloid Interface Sci.* 179:298–310.
19. Narayan, V., S. Ramaswamy, and N. Menon. 2007. Long-lived giant number fluctuations in a swarming granular nematic. *Science.* 317:105–108.
20. Hoffmann, E. K., and L. O. Simonsen. 1989. Membrane mechanisms in volume and pH regulation in vertebrate cells. *Physiol. Rev.* 69:315–382.
21. Henkes, S., Y. Fily, and M. C. Marchetti. 2011. Active jamming: self-propelled soft particles at high density. *Phys. Rev. E Stat. Nonlin. Soft Matter Phys.* 84:040301.
22. Deforet, M., M. C. Parrini, …, P. Silberzan. 2012. Automated velocity mapping of migrating cell populations (AVeMap). *Nat. Methods.* 9:1081–1083.
23. Schaller, V., and A. R. Bausch. 2013. Topological defects and density fluctuations in collectively moving systems. *Proc. Natl. Acad. Sci. USA.* 110:4488–4493.
24. Dermietzel, R., and D. C. Spray. 1993. Gap junctions in the brain: where, what type, how many and why? *Trends Neurosci.* 16:186–192.
25. Evans, W. H., and P. E. Martin. 2002. Gap junctions: structure and function (Review). *Mol. Membr. Biol.* 19:121–136.
26. Meyer, D. J., S. B. Yancey, and J. P. Revel. 1981. Intercellular communication in normal and regenerating rat liver: a quantitative analysis. *J. Cell Biol.* 91:505–523.
27. Caspar, D. L. D., D. A. Goodenough, …, W. C. Phillips. 1977. Gap junction structures. I. Correlated electron microscopy and x-ray diffraction. *J. Cell Biol.* 74:605–628.
28. Bennett, M. V., and V. K. Verselis. 1992. Biophysics of gap junctions. *Semin. Cell Biol.* 3:29–47.
29. Giaume, C., C. Sahuquillo, …, H. Korn. 1986. Evidence for ionic coupling between MDCK cells at non-confluent and confluent stages of culture. *Biol. Cell.* 57:33–38.
30. Discher, D. E., P. Janmey, and Y. L. Wang. 2005. Tissue cells feel and respond to the stiffness of their substrate. *Science.* 310:1139–1143.
31. Larsen, W. J. 1977. Structural diversity of gap junctions. A review. *Tissue Cell.* 9:373–394.
32. Dullien, F. A. 1991. Porous Media: Fluid Transport and Pore Structure. Academic Press, New York.
33. Howard, J. 2001. Mechanics of Motor Proteins and the Cytoskeleton. Sinauer, Sunderland, MA.
34. Satcher, Jr., R. L., and C. F. Dewey, Jr. 1996. Theoretical estimates of mechanical properties of the endothelial cell cytoskeleton. *Biophys. J.* 71:109–118.
35. Medalia, O., I. Weber, …, W. Baumeister. 2002. Macromolecular architecture in eukaryotic cells visualized by cryoelectron tomography. *Science.* 298:1209–1213.
36. Charras, G. T., J. C. Yarrow, …, T. J. Mitchison. 2005. Non-equilibration of hydrostatic pressure in blebbing cells. *Nature.* 435:365–369.
37. Bursac, P., G. Lenormand, …, J. J. Fredberg. 2005. Cytoskeletal remodeling and slow dynamics in the living cell. *Nat. Mater.* 4:557–561.
38. Timbs, M. M., and K. R. Spring. 1996. Hydraulic properties of MDCK cell epithelium. *J. Membr. Biol.* 153:1–11.
39. Pierce, S. K., and A. D. Politis. 1990. $Ca^{2+}$-activated cell volume recovery mechanisms. *Annu. Rev. Physiol.* 52:27–42.

**Supporting Material**

Cell Volume Fluctuations in MDCK Monolayers

Steven M. Zehnder,[*] Melanie Suaris,[†] Madisonclaire M. Bellaire,[‡] and Thomas E. Angelini,[*†¶]

[*]Department of Mechanical and Aerospace Engineering, University of Florida, Gainesville, USA; [†]J. Crayton Pruitt Family Department of Biomedical Engineering, University of Florida, Gainesville, USA; [‡]Department of Physics, University of Florida, Gainesville, USA; [¶]Institute for Cell Engineering and Regenerative Medicine, University of Florida, Gainesville, USA

## Movie S1

Fluctuations in the projected areas of cells can be seen in time-lapse. At any instant, regions of low number density composed of large cells coexist near regions of high number density composed of small cells. Over time, single cells fluctuate in projected area, sometimes doubling or tripling in size. Cell divisions appear as extremely rapid reductions in cell area compared to area fluctuations between divisions. The fast decrease in area of dividing cells facilitates their identification and rejection from analysis. Scalebar 150 μm.

## Cell Culture Protocols and Experimental Details

MDCK epithelial cell layers are plated on glass-bottomed culture dishes coated with collagen I. Cells are cultured in Dulbecco's Modified Eagle Medium (DMEM), 5% fetal bovine serum, 1% penicillin-streptomycin, and maintained at 37 °C and 5% $CO_2$. For experiments in which cells are fluorescently dyed, cells are treated with 15 μM 5-chloromethylfluorescein diacetate (CMFDA) in serum-free DMEM and 0.15% DMSO for 30 minutes, then returned to full serum-containing DMEM and immediately imaged in time-lapse. For Myosin II inhibition experiments, growth media supplemented with 100μM blebbistatin is used. Cells are transferred to an inverted microscope with automated shuttering and full environmental control. Low light levels are maintained by using a 10% neutral density filter in line with the fluorescence lamp and by opening the shutter for less than 100ms every minute for 9 hours. To eliminate z-drift after a focal plane is chosen, we use an interferometric objective positioning system (Nikon Perfect Focus), which does not rely on any image-based auto-focusing algorithms and maintains focus within a few nanometers along the optical axis. Volume fluctuation measurements of cells with and without blebbistatin treatment were repeated three times, producing consistent results.

Cells are plated as circular islands approximately 5mm in diameter. Cells are deposited at the minimum confluent density, which is just dense enough such that no open space is observed within the layer. Imaging is performed away from the immediate edge of the island in a region where island expansion and cell proliferation nearly balance, and consequently the average cell density rises very slowly. We measured the cell division rate in this system, finding a division time of approximately 40 hours, in agreement with our previous studies. Dividing cells are identified by a large, rapid drop in measured area over the course of about 10-20 minutes; dividing cells are not included in the analysis. A relatively small change in cell density over time is observed at the large scale by measuring the average cell area at each time point (Fig. S1). Traces of individual cell area also show no dramatic transient behavior, though each cell fluctuates substantially over time (Fig. S2). These strong fluctuations in cell area are coupled to local fluctuations in multicellular motion, though we observe no significant collective migration over lengthscales exceeding approximately 200 μm (Video S1). The oscillatory nature of single cell area, averaged over hundreds of cell area traces, is captured by the autocorrelation function, described in the manuscript. In Fourier analysis of signals, the lowest measurable frequency has a corresponding period of twice the sample duration. Thus, for each single 9 hour cell measurement, the minimum measurable frequency increment is 1/18 $h^{-1}$. The frequency of a 4 hour period is 1/4 $h^{-1}$, 4.5 times the lowest measureable frequency. The frequency of a 6 hour period is 1/6 $h^{-1}$, 3 times the lowest measurable frequency. Thus, the period of oscillation measured from correlation functions or Fourier spectra are not limited by the duration of the experiments.

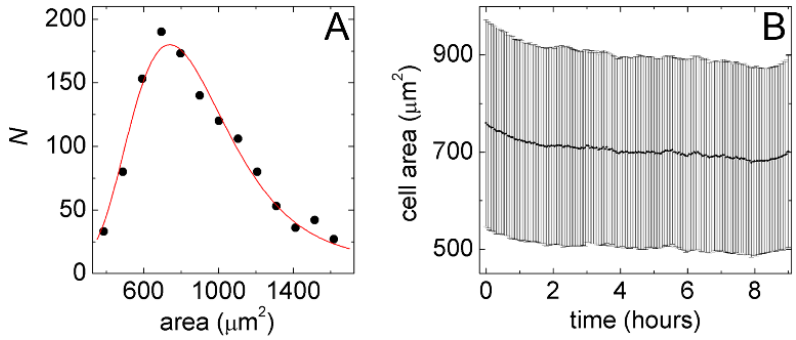


**Figure S1.** Within each collected frame, the cell area histogram is skewed and is well described by a log-normal distribution (A, dots are data, red line is a log-normal distribution fit). To measure a representative cell area within the monolayer at each time, we estimate the location of the peak in each histogram and a coefficient of variation by using log-normal statistics. The resulting plot of cell area versus time shows a small decrease in average cell area from about 750 $\mu m^2$ to just below 700 $\mu m^2$, with a very large variation in size at all times (B).

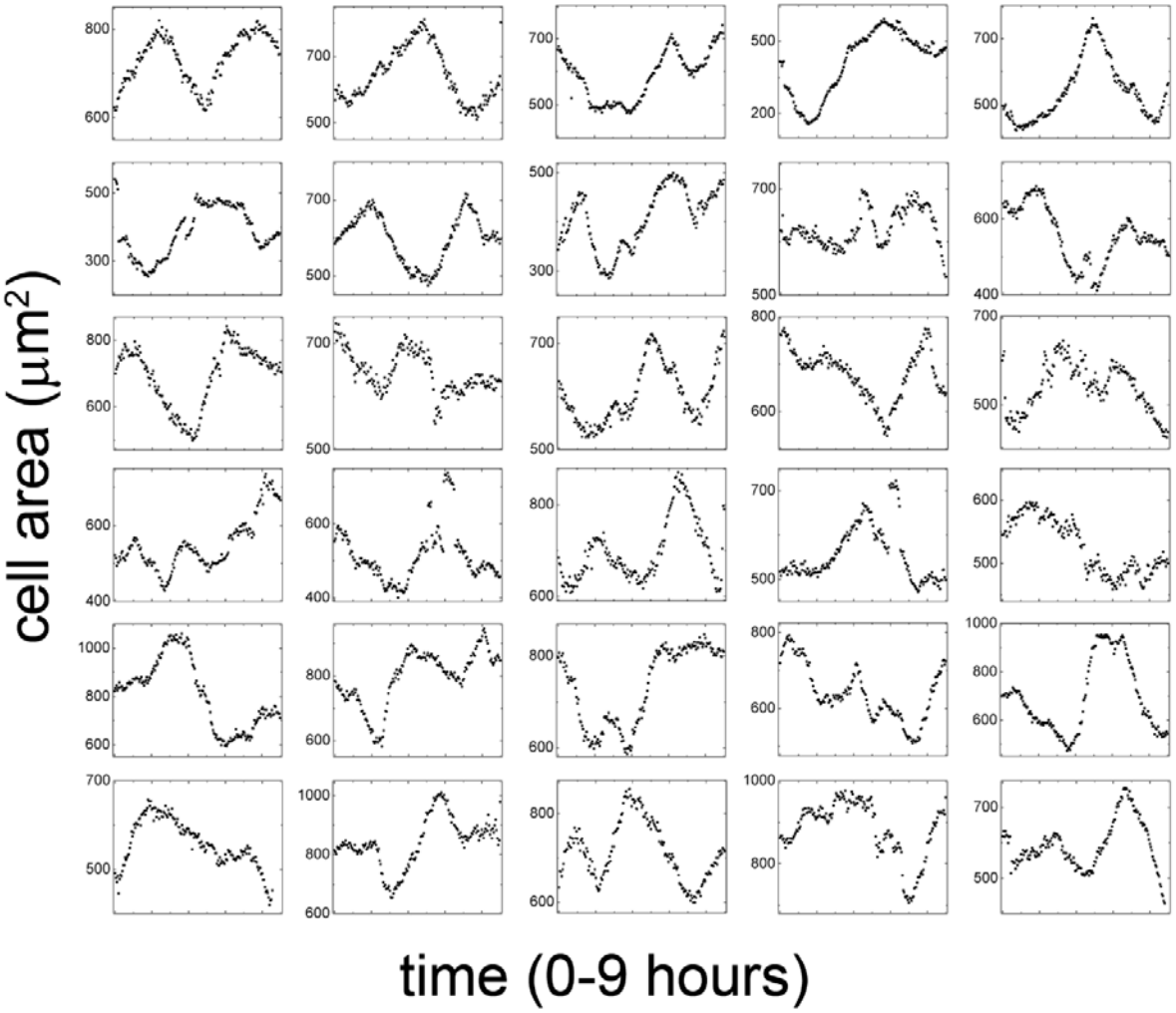


**Figure S2.** The typical cell fluctuates in area by about ±20% every four hours, performing a full oscillation in about 1/10 of the typical cell division time. Thirty traces of different cell areas versus time show the general oscillatory fluctuating behavior, but individual cells can fluctuate by much more or less than the average, and also oscillate at different rates.

## Cell Volume, Area, and Thickness

Measurements of cell thickness variation in time and space, described in the manuscript text, demonstrate that cell thickness fluctuations are small compared to cell area fluctuations. The disparity between cell area fluctuations and cell thickness fluctuations reveals that cell volume fluctuations accompany area fluctuations, though it is unclear whether spreading cells become thinner or thicker, even if the change is small. To test whether spreading cells become thinner and contracting cells become thicker, conserving some fraction of volume, we follow the area, thickness, and volume of several cells in the confocal microscope over time. The cell boundary at each time point is identified by computing an average intensity projection along the z-axis; since a great number of cells possess nearly vertical interfaces, their boundaries are easily identified. The height at every location within the cell boundary is measured in the same way as described in the manuscript, and an average is taken to determine cell thickness at each point in time. The product of the X-Y pixel size and the height at any single location within the cell boundary produces a volume element; the volume of the cell is computed from the sum of all volume elements within the cell boundary.

We find that the instantaneous variation in height across a single cell surface is larger than the change in average height over time. Surprisingly, when tracking changes in a cell with strongly decreasing area, we find that the cell thickness also decreases, exhibiting no sign of volume conservation at all. By contrast, a cell with moderately decreasing area thickens, exhibiting volume conservation. A cell with increasing area was found to exhibit no clear change in thickness. Thus, plots of cell thickness versus volume show no systematic correlation across these different cells. However, plots of area versus volume show strong correlations, suggesting that fluctuations in volume may be approximated by fluctuations in area (Fig. S3).

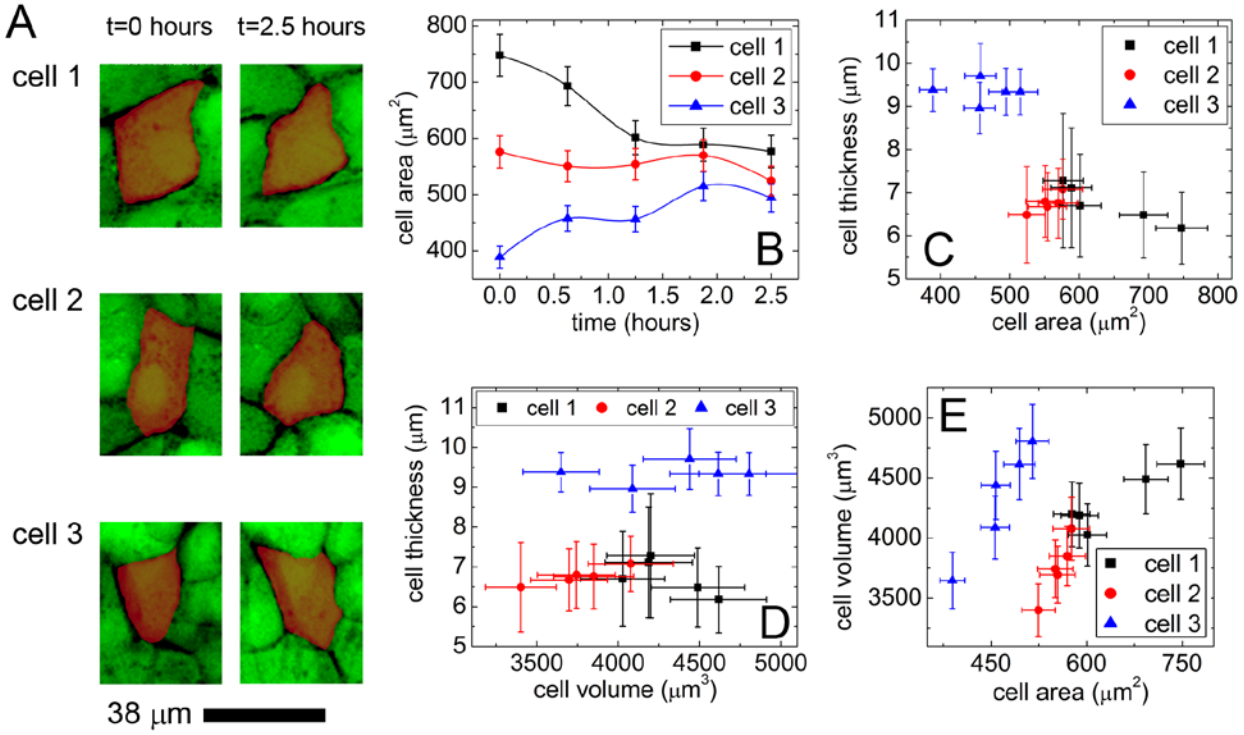


**Figure S3.** Cell boundaries are identified in z-projections of confocal stacks (A). The cells exhibit different variations in area over time (B, Errorbars: uncertainty estimate of area for precision of 1 pixel). Cell 1 decreases in area and decreases in thickness; cell 2 decreases in area and increases in thickness; cell 3 increases in area and does not change thickness (C, bars are standard deviation of height across the cell surface). There is no systematic change in thickness with volume (D), yet there are strong, systematic correlations between cell area and cell volume (E, volume errorbars: combination of height and area error estimates).

## Spatial Correlations in Cell Density and Area

Heterogeneity in cell size appears to occur over a characteristic multi-cellular lengthscale. To quantify these apparent spatial correlations in cell density, we compute a density-density autocorrelation function. With the Voronoi tessellation analysis described in the main text, the area of every cell within the field of view is computed, and a spatial map of area is constructed. The reciprocal of this area map is a map of local number density of cells. We compute the density-density autocorrelation function in 2D, $C_{\sigma\sigma}(\mathbf{R}) = \langle \sigma(\mathbf{r})\sigma(\mathbf{r}+\mathbf{R}) \rangle_{\mathbf{r}}$, where $\sigma$ is the number density and the angle brackets indicate an average over all locations in space. The 2D correlation function is azimuthally averaged to produce a simple 1D correlation function, $C_{\sigma\sigma}(R) = \langle C_{\sigma\sigma}(\mathbf{R}) \rangle_{\phi}$. We find that $C_{\sigma\sigma}$ decays rapidly out to approximately 75 microns, or 3-4 cell lengths. At larger distances, $C_{\sigma\sigma}$ exhibits a rise and a peak at a lengthscale of about 200 μm, or ten cell lengths. Thus, cell area and number density exhibit a spatial fluctuation on multi-cellular lengthscales. This lengthscale is comparable to spatial correlation lengths observed in migration velocity fields. Thus, a strong coupling between cell density fluctuations and spatial correlation in migration velocity is likely to occur here, and insight may be found in previous work in active particulate systems (2-4).

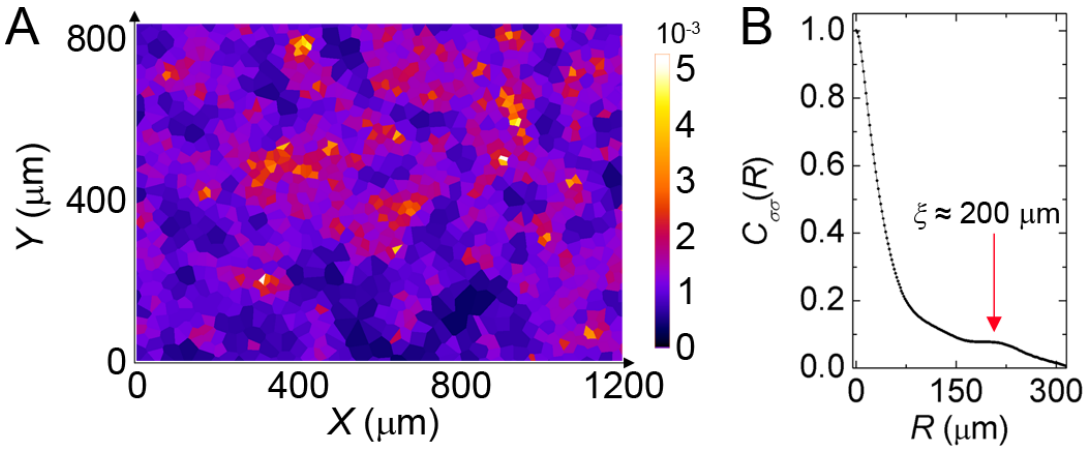


**Figure S4.** Voronoi tessellations are generated from cell nuclei positions, and individual cell areas are approximated by the corresponding Voronoi cell areas. Cell density, $\sigma$, is computed from the reciprocal of cell area (B, intensity bar units are cells per μm$^2$). The density-density autocorrelation function, $C_{\sigma\sigma}(R)$ exhibits a small peak at $R$ = 200 μm, corresponding to the spacing between regions of similar density.

## Gap Junction Permeability

Large assemblies of fluid channels, known as gap junctions, constitute several percent of the cell-cell interface, connecting neighboring cells in tissues and monolayers (5-8). The resistance to pressure-driven flow through gap junctions can be estimated from the dimensions of their channels and the number of open channels that connect cells. From gap junction conductance measurements of MDCK cells and single gap junction channel conductance we estimate that a typical MDCK cell is connected to its neighbors through approximately 2000 open gap junction channels (9,10). Approximating transport through these channels as Poiseuille flow, we predict a permeability, $k = \left(N_c \pi D^4\right) / \left(128 \eta L\right)$, where $N_c$ is the number of channels per cell, $D$ is the diameter of each channel, $\eta$ is the fluid viscosity, and $L$ is the channel length. For a fluid with the viscosity of water driven through channels of diameter, $D$ = 2 nm, and length, $L$ =16 nm, we find $k$ = 0.06 μm$^3$ kPa$^{-1}$ s$^{-1}$. A cell with this permeability could expel 20% of its own volume in two hours by generating only 1.1 kPa of excess pressure, relative to its neighbors. Comparable levels of spatial variability in cell generated normal-stress have been measured in epithelial, endothelial, and cancer cell monolayers. These back-of-the-envelope estimates suggest that the levels of pressure required to drive intercellular fluid flow are modest, and given the ubiquity of gap junctions and contractile force generation in tissue cells, cell volume changes may drive intercellular fluid flow in many systems (5,11,12).

### Cytoskeleton Permeability

In order for fluid to flow from cell-to-cell, it must also traverse the cytoskeleton. The permeability of any dense polymer network, including the cytoskeleton, is expected to be excessively low for pressure driven flow, limited by the small mesh-size. To test the cytoskeleton's potential to limit intercellular flow, we estimate the effective permeability of the cytoskeleton to be $k = A\xi^2 / \eta L$, where $A$ is the cell cross sectional area in profile, $\xi$ is the network mesh-size, $\eta$ is the fluid viscosity, and $L$ is the lateral lengthscale over which the fluid must flow (13). For a cell with an area in profile, $A = hL$, a cell height, $h$ = 7 μm, a mesh size of 100 nm (14-16), and a viscosity, $\eta$ = 0.89 mPa s, we estimate an effective cytoskeletal permeability of $8\times10^4$ $\mu m^3$ $kPa^{-1}$ $s^{-1}$, many orders of magnitude larger than the estimated single cell, gap junction permeability. Previous work showed that over short time-scales, less than about a minute, the cytoskeleton permeability limits flow and poroelastic effects dominate (17). However, in our work we observe volume changes over the course of hours and we expect permeability to be further increased over longer time-scales; the cytoskeleton is in constant flux, maintaining cytoskeletal tension while remodeling over times shorter than the volume fluctuations observed here (18).

### Membrane and Aquaporin Permeability

Isolated cells under isotonic conditions maintain a constant volume, although applied osmotic pressure can drive fluid across the cell membrane or through aquaporins, generating cell volume change (1). The hydraulic permeability of individual MDCK cells has been measured by monitoring cell volume change under increased osmotic pressure (19). An increase in the osmotic pressure of the growth media by about 200kPa, or 80 mOsm/kg, causes the cells to shrink rapidly over the course of a few minutes, and the MDCK permeability is found to be $2\times10^{-8}$ cm $s^{-1}$ $mOsm^{-1}$ kg. (19). To compare to the permeability estimates above, we multiply this permeability by the measured projected cell area of 700 $\mu m^2$ and convert units, finding a permeability of 0.06 $\mu m^3$ $kPa^{-1}$ $s^{-1}$. Interestingly, this permeability is the same as the permeability of cells for flow through gap junctions. When osmotic pressure is applied to cells, they respond by rapidly transferring ions across the membrane with ion pumps, driving water across the cell membrane, recovering most of their equilibrium volume within few minutes (20). This suggests that cells can generate osmotic pressures of at least 100kPa by driving ion transport. Thus, these simple estimates suggest the possibility that cells in monolayers generate the volume fluctuations that we observe here if ion transport oscillates regularly over the course of several hours.

## SUPPLEMENTARY REFERENCES


1. Hoffmann, E. K. and L. Simonsen. 1989. Membrane mechanisms in volume and pH regulation in vertebrate cells. Physiol Rev 69:315-382.

2. Henkes, S., Y. Fily, and M. C. Marchetti. 2011. Active jamming: Self-propelled soft particles at high density. Physical Review E 84:040301.

3. Deforet, M., M. C. Parrini, L. Petitjean, M. Biondini, A. Buguin, J. Camonis, and P. Silberzan. 2012. Automated velocity mapping of migrating cell populations (AVeMap). Nature methods 9:1081-1083.

4. Schaller, V. and A. R. Bausch. 2013. Topological defects and density fluctuations in collectively moving systems. Proceedings of the National Academy of Sciences 110:4488-4493.

5. Dermietzel, R. and D. C. Spray. 1993. Gap junctions in the brain: where, what type, how many and why? Trends in Neurosciences 16:186-192.

6. Evans, W. H. and P. E. Martin. 2002. Gap junctions: structure and function (Review). Molecular membrane biology 19:121-136.

7. Meyer, D. J., S. B. Yancey, and J. P. Revel. 1981. Intercellular communication in normal and regenerating rat liver: a quantitative analysis. The Journal of Cell Biology 91:505-523.

8. Caspar, D. L. D., D. A. Goodenough, L. Makowski, and W. C. Phillips. 1977. Gap Junction Structures: I. Correlated Electron Microscopy and X-Ray Diffraction. The Journal of Cell Biology 74:605-628.

9. Bennett, M. and V. Verselis. 1992. Biophysics of gap junctions. Seminars in cell biology 3:29-47.

10. Giaume, C., C. Sahuquillo, D. Louvard, and H. Korn. 1986. Evidence for ionic coupling between MDCK cells at non-confluent and confluent stages of culture. Biology of the Cell 57:33-38.

11. Discher, D. E., P. Janmey, and Y.-l. Wang. 2005. Tissue Cells Feel and Respond to the Stiffness of Their Substrate. Science 310:1139-1143.

12. Larsen, W. J. 1977. Structural diversity of gap junctions. A review. Tissue and Cell 9:373-394.

13. Dullien, F. A. 1991. Porous media: fluid transport and pore structure: Academic press.

14. Howard, J. 2001. Mechanics of motor proteins and the cytoskeleton.

15. Satcher Jr, R. L. and C. F. Dewey Jr. 1996. Theoretical estimates of mechanical properties of the endothelial cell cytoskeleton. Biophysical journal 71:109-118.

16. Medalia, O., I. Weber, A. S. Frangakis, D. Nicastro, G. Gerisch, and W. Baumeister. 2002. Macromolecular architecture in eukaryotic cells visualized by cryoelectron tomography. Science 298:1209-1213.

17. Charras, G. T., J. C. Yarrow, M. A. Horton, L. Mahadevan, and T. Mitchison. 2005. Non-equilibration of hydrostatic pressure in blebbing cells. Nature 435:365-369.

18. Bursac, P., G. Lenormand, B. Fabry, M. Oliver, D. A. Weitz, V. Viasnoff, J. P. Butler, and J. J. Fredberg. 2005. Cytoskeletal remodelling and slow dynamics in the living cell. Nature materials 4:557-561.

19. Timbs, M. and K. Spring. 1996. Hydraulic properties of MDCK cell epithelium. The Journal of membrane biology 153:1-11.

20. Pierce, S. K. and A. D. Politis. 1990. Ca2+-activated cell volume recovery mechanisms. Annual review of physiology 52:27-42.